

Supporting Information

Single-cluster Au as an Usher for Deeply Cyclable Li Metal Anode

Tingzhou Yang^{1, 2}, Tao Qian^{1, *}, Xiaowei Shen¹, Mengfan Wang¹, Sisi Liu¹, Jun Zhong³, Chenglin Yan^{1, *}, Federico Rosei^{2, *}

¹College of Energy, Soochow University, Suzhou 215006, China.

²Institut National de la Recherche Scientifique, Centre Énergie, Matériaux et Télécommunications, 1650 Boulevard Lionel Boulet, J3X 1S2 Varennes, Québec, Canada.

³Institute of Functional Nano and Soft Materials (FUNSOM), Jiangsu Key Laboratory for Carbon-Based Functional Materials and Devices, Soochow University, Suzhou 215123, China.

*Correspondence and requests for materials should be addressed to T.Q. (email: tqian@suda.edu.cn), F.R. (email: rosei@emt.inrs.ca) or to C.L.Y. (email: c.yan@suda.edu.cn).

Table S1. Summary of the reported literature on different types of Au or Ag modified current collector.^{S1-S5}

Current collector	CE at 0.5 mA cm ⁻²	CE at 1.0 mA cm ⁻²	CE at 5.0 mA cm ⁻²	maximal life time	maximal deeply cyclable capacity
Carbon spheres with Au nanoparticles	93%	-	-	300 cycles	2.0 mAh cm ⁻²
Au modified carbon fiber matrix	-	99.2%	98%	400 cycles	5.0 mAh cm ⁻²
Au nanoparticles pillared RGO	98.70%	~98%	-	200 cycles	5.0 mAh cm ⁻²
Ag coated carbon fiber framework	-	-	-	200 cycles	10.0 mAh cm ⁻²
Ag nanoparticles anchored on carbon nanofiber	98%	-	-	200 cycles	2.0 mAg cm ⁻²
Our strategy	99.82%	99.6%	99.17%	900 cycles	20.0 mAh cm ⁻²

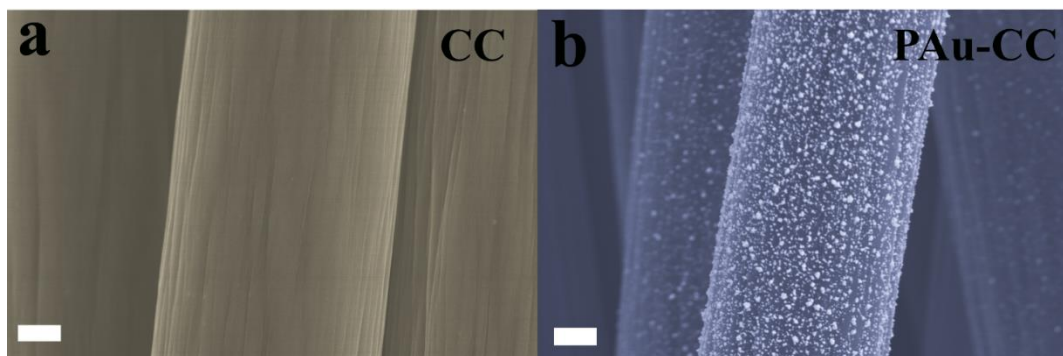


Figure S1. (a) SEM image of CC. (b) SEM image of PAu-CC, which shows the Au nanoparticle dispersed on the surface of CC. Scale bar, 10 μm .

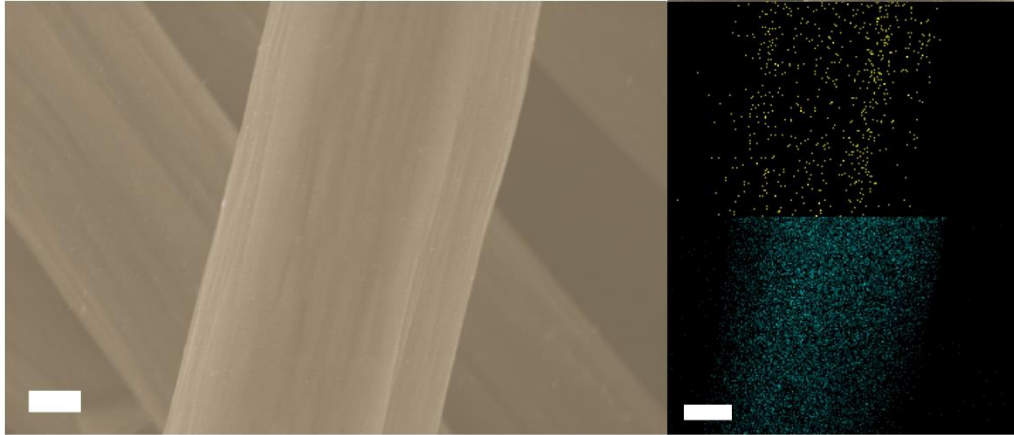


Figure S2. SEM images of SCAu-CC. Examination of the corresponding EDS mapping of Au and C reveals the homogeneous distribution of single-cluster Au on the carbon skeleton. Scale bar, 10 μm .

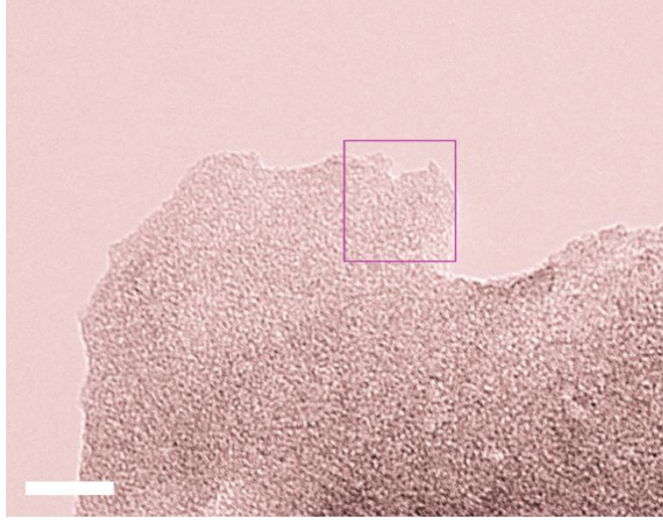


Figure S3. TEM image of SCAu-CC, and the selection of EELS mapping. Scale bar, 20nm.

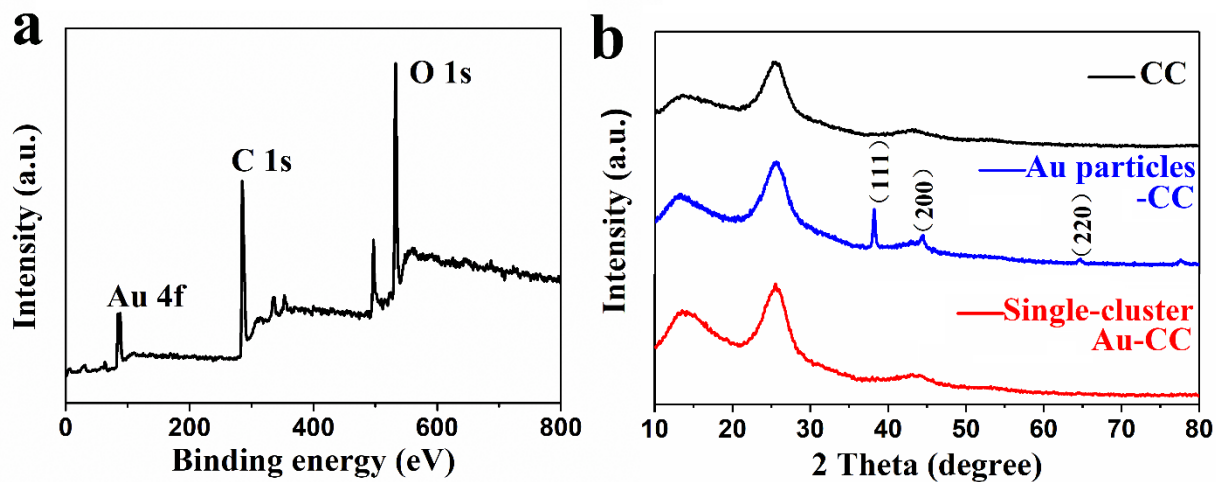


Figure S4. (a) X-ray photoelectron spectroscopy spectrum of SCAu-CC. (b) Comparison of X-ray diffraction patterns of CC, Pau-CC and SCAu-CC.

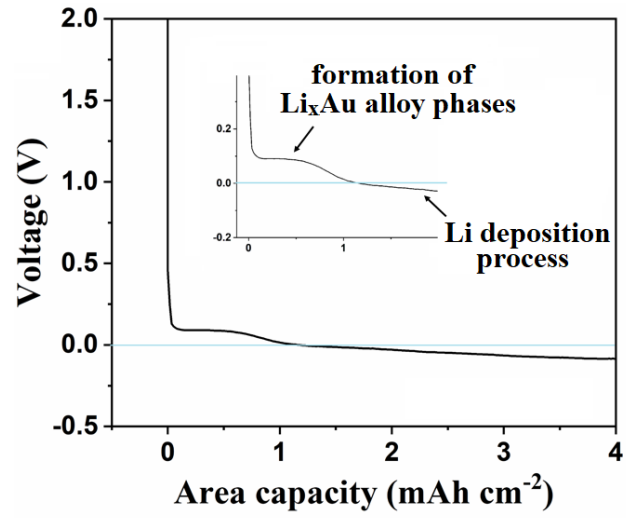


Figure S5. Voltage profiles of galvanostatic Li deposition on the SCAu-CC, which shows unique nucleation mechanism during first Li plating process.

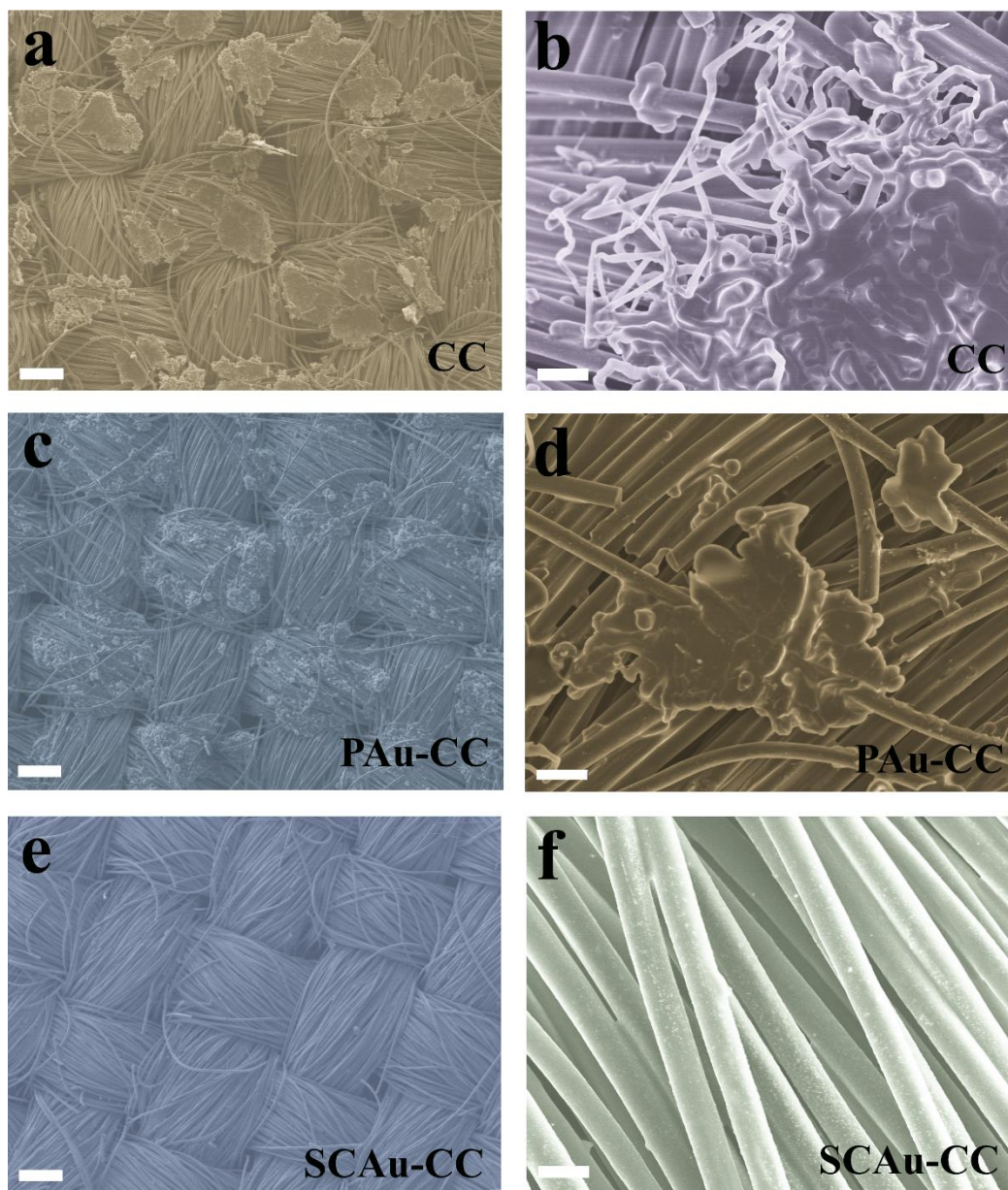


Figure S6. Morphology characterization by SEM images of (a,b) CC, (c,d) PAu-CC and (e,f) SCAu-CC after after plating 6.0 mAh cm^{-2} of Li metal. Scale bar, $500 \mu\text{m}$ and $50 \mu\text{m}$.

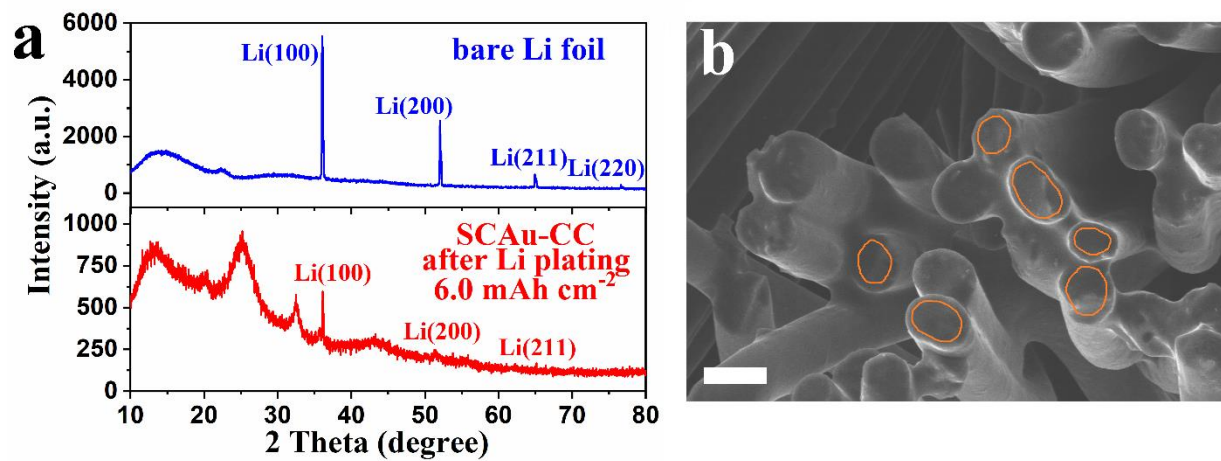


Figure S7. (a) Comparison of XRD patterns of bare Li foil and Li-SCAu-CC. Both of them exhibit the peaks centered at 36° (100), 52° (200) and 65° (211), demonstrating the successful Li plating on SCAu-CC. (b) The cross-section SEM view of the Li-SCAu-CC (6.0 mAh cm⁻²).

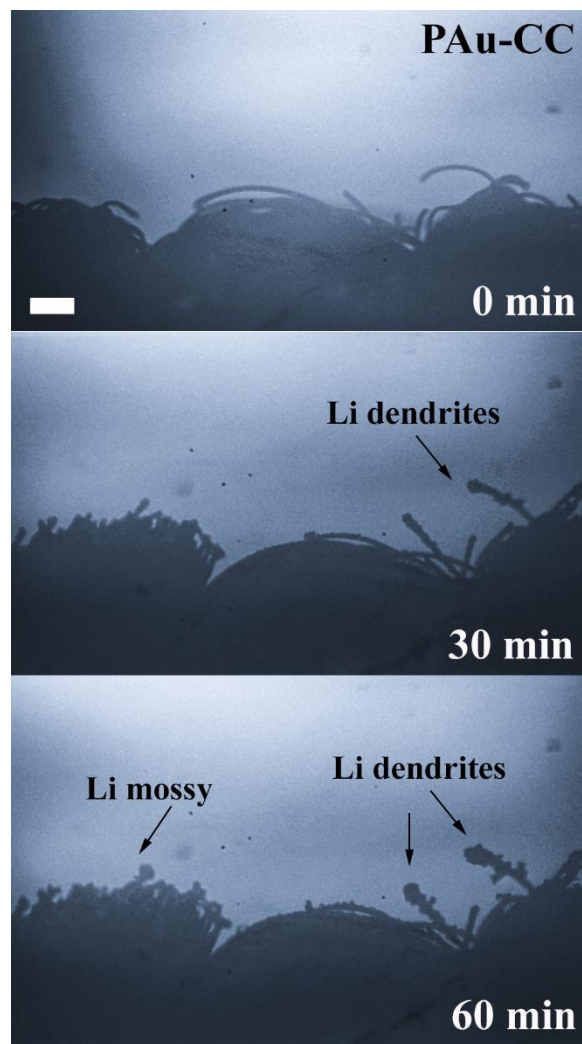


Figure S8. In situ optical microscopy observations of Li deposition process in PAu-CC.

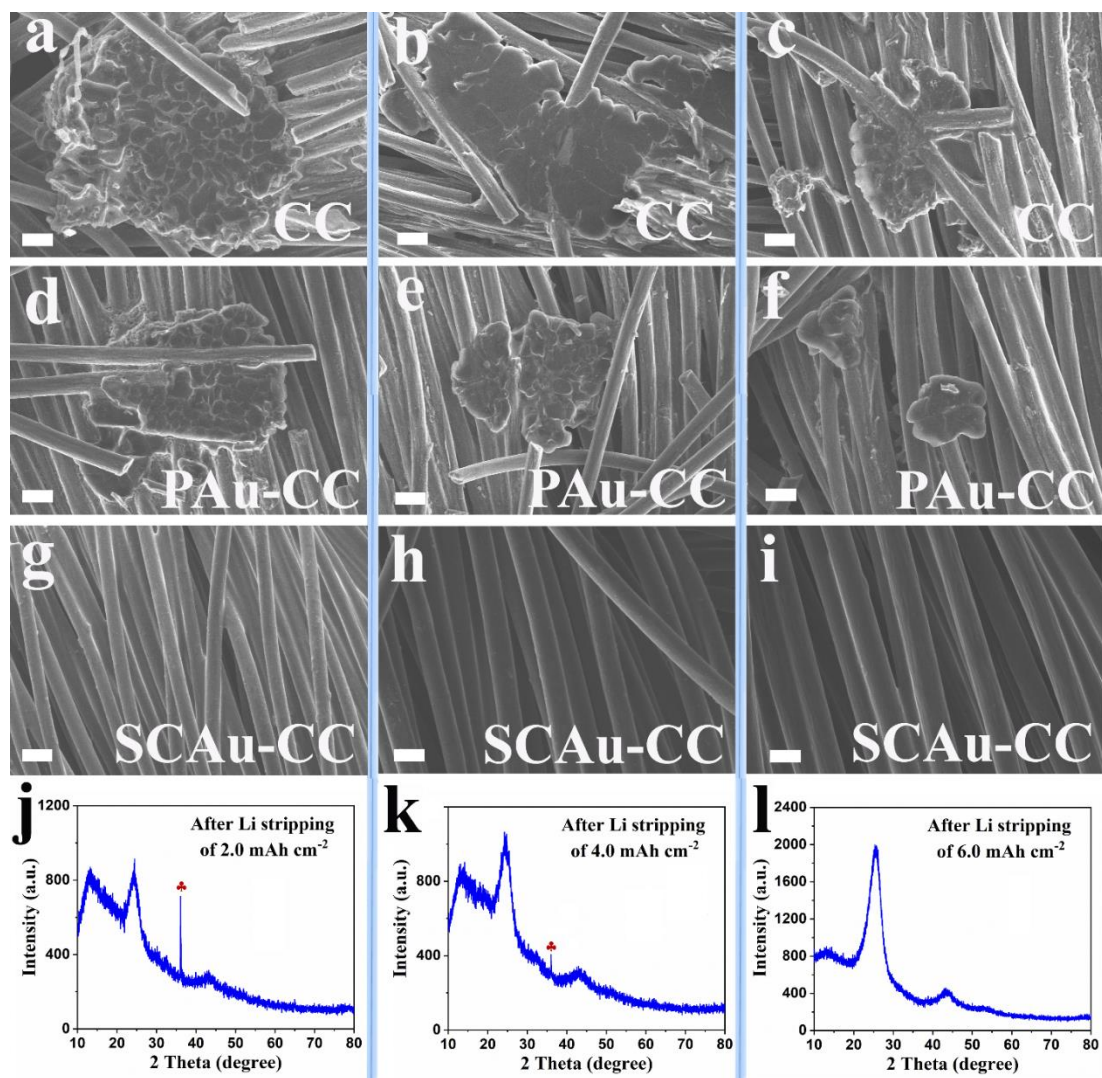


Figure S9. The SEM analysis of CC electrodes after (a) 2.0, (c) 4.0, and (e) 6.0 mAh cm⁻² of Li stripping. The morphologies of PAu-CC electrodes after (b) 2.0, (e) 4.0, and (f) 6.0 mAh cm⁻² of Li stripping. The morphologies and corresponding XRD patterns of Li-SCAu-CC (6.0 mAh cm⁻²) electrodes after (g, j) 2.0, (h, k) 4.0, and (i, l) 6.0 mAh cm⁻² of Li stripping.

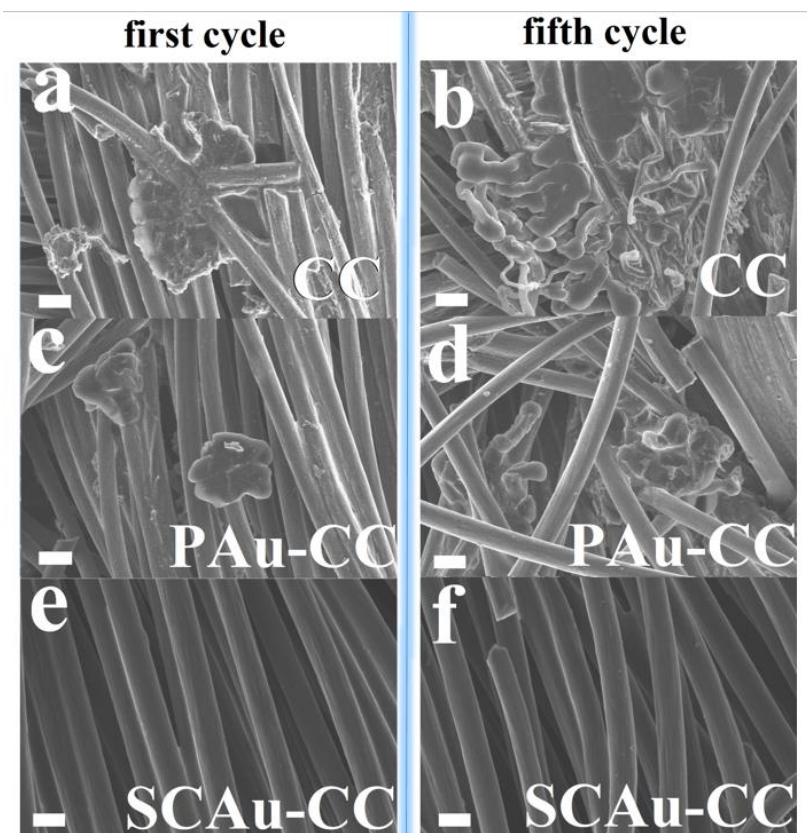


Figure S10. Characterization of Li metal anodes after Li stripping process at a current density of 1.0 mAh cm^{-2} with an area capacity of 6.0 mAh cm^{-2} . SEM images of (a) CC, (b) PAu-CC, and (c) SCAu-CC electrodes for the first cycle. SEM images of (d) CC, (e) PAu-CC, and (f) SCAu-CC electrodes after fifth Li stripping process. Scale bars: $10 \mu\text{m}$.

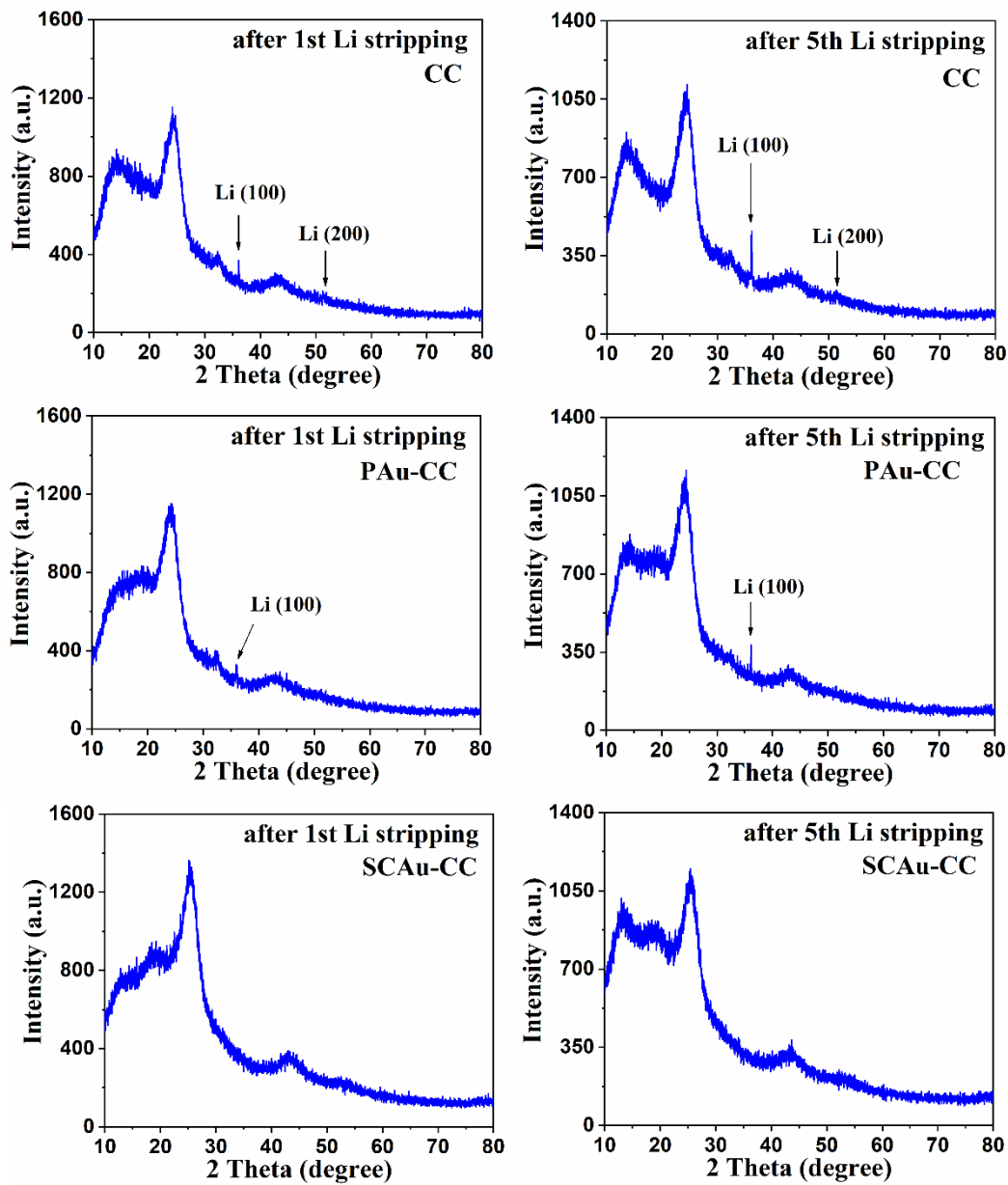


Figure S11. Comparison of XRD patterns of (a,b) CC, (c,d) PAu-CC and (e,f) SCAu-CC after the first cycle and the fifth cycle of Li stripping process.

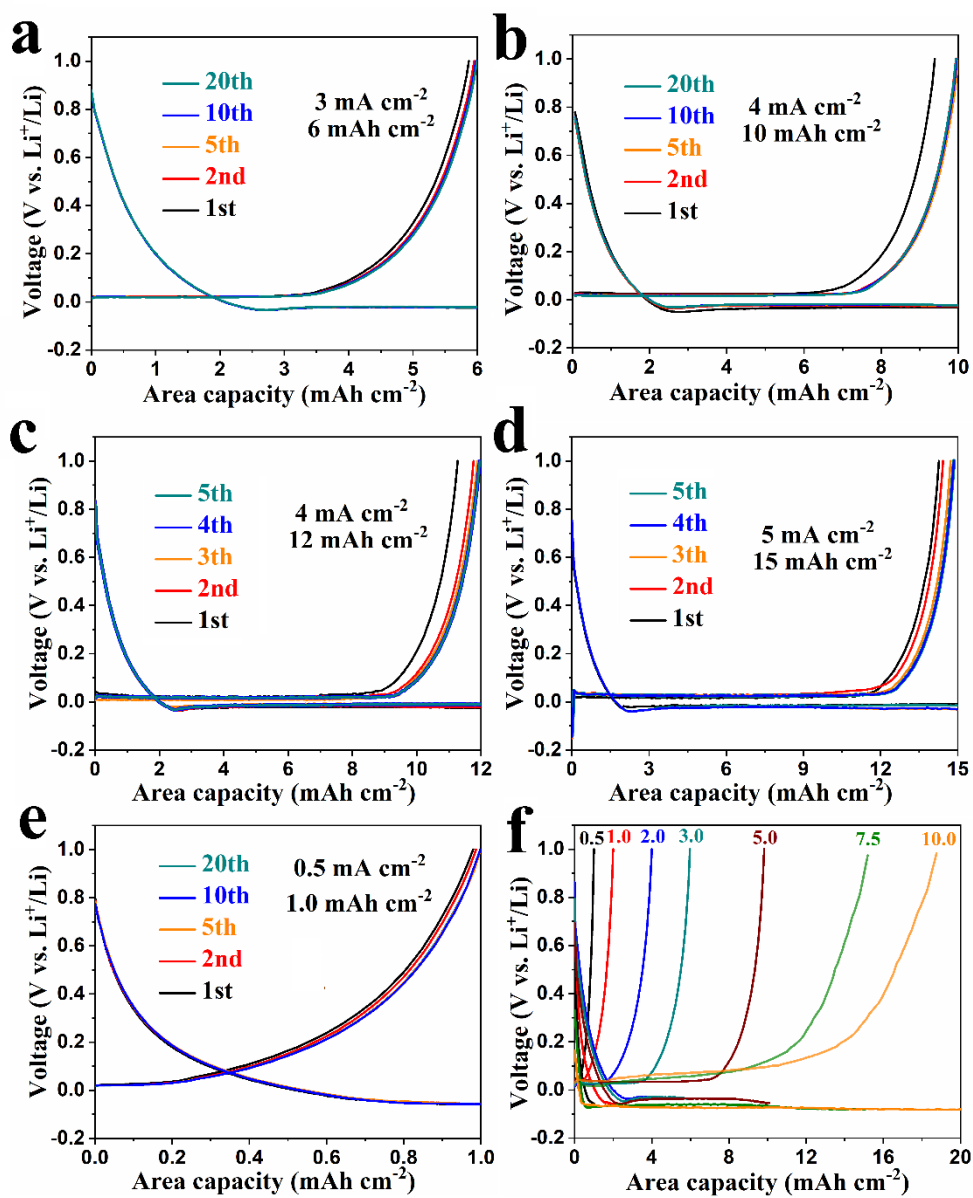


Figure S12. Voltage profiles of different Li plating/stripping process for SCAu-CC at different current density with an area capacity of (a) 6.0 mAh cm^{-2} , (b) 10.0 mAh cm^{-2} , (c) 12.0 mAh cm^{-2} , (d) 15.0 mAh cm^{-2} , and (e) 1.0 mAh cm^{-2} . (f) Voltage profiles of Li plating/stripping process at different current densities ($0.5, 1.0, 2.0, 5.0, 7.5, 10.0 \text{ mA cm}^{-2}$).

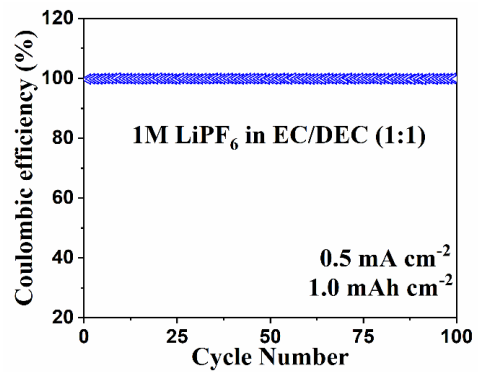


Figure S13. Electrochemical characterization of the SCAu-CC electrode with for Li plating and stripping process by the using of carbonate-based electrolyte.

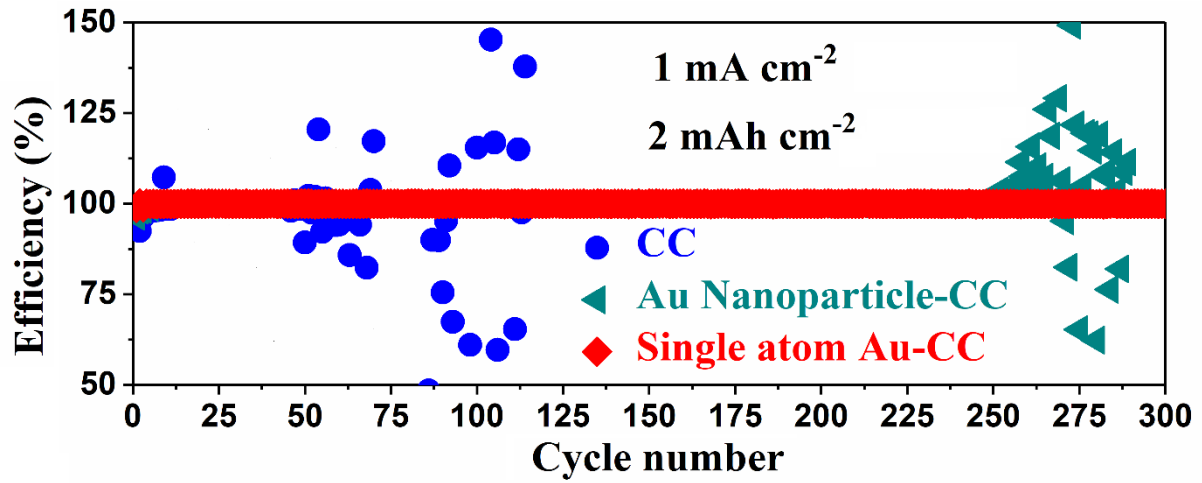


Figure S14. Comparison of CE of Li plating/stripping between CC, PAu-CC and SCAu-CC with areal capacity of 1.0 mAcm⁻² at a current density of 2.0 mA cm⁻².

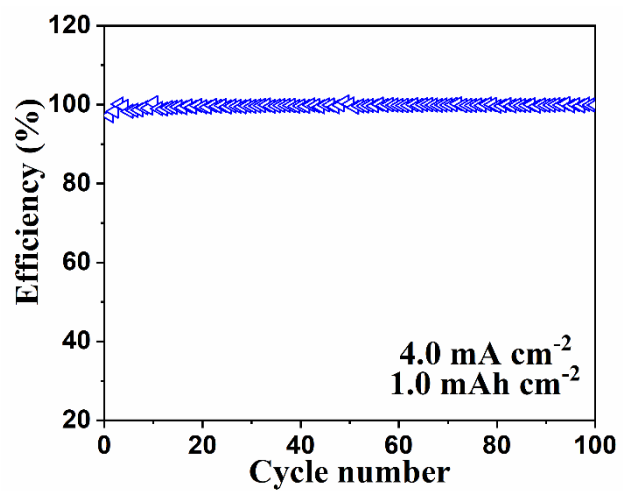


Figure S15. Coulombic efficiency of SCAu-CC at a high current density of 4.0 mA cm^{-2} and a low capacity of 1.0 mAh cm^{-2}

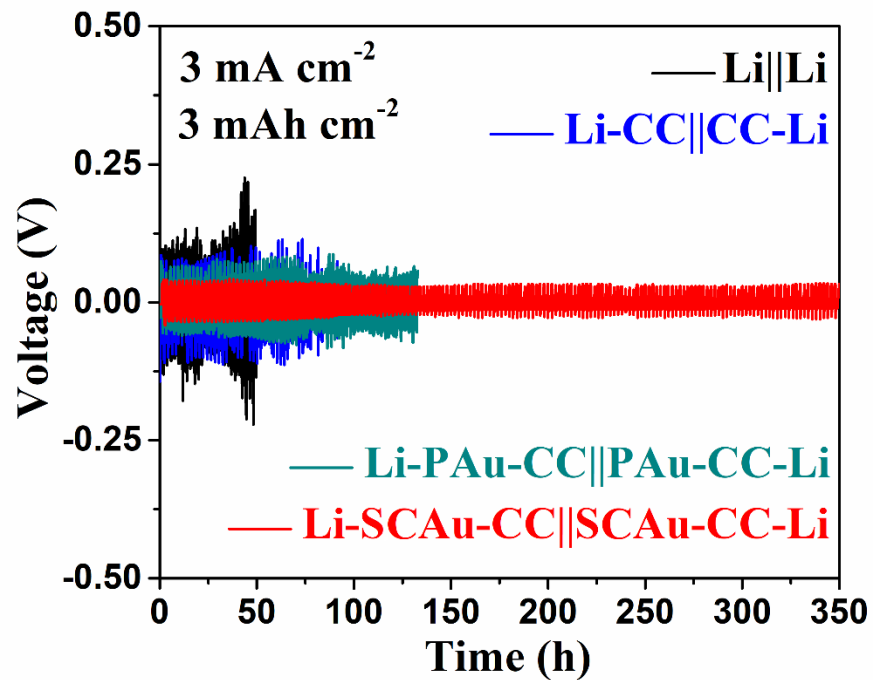


Figure S16. Galvanostatic Li plating/stripping profiles of symmetric cells with different anode with areal capacity of 3.0 mAh cm^{-2} at a current density of 3.0 mA cm^{-2} .

References:

- S1 K. Yan, Z. Lu, H.-W. Lee, F. Xiong, P.-C. Hsu, Y. Li, J. Zhao, S. Chu and Y. Cui, *Nat Energy*, 2016, **1**, 359.
- S2 J. Xiang, L. Yuan, Y. Shen, Z. Cheng, K. Yuan, Z. Guo, Y. Zhang, X. Chen and Y. Huang, *Adv. Energy Mater.*, 2018, **8**, 1802352.
- S3 C. Yang, Y. Yao, S. He, H. Xie, E. Hitz and L. Hu, *Adv. Mater.*, 2017, **29**, 1702714.
- S4 R. Zhang, X. Chen, X. Shen, X.-Q. Zhang, X.-R. Chen, X.-B. Cheng, C. Yan, C.-Z. Zhao and Q. Zhang, *Joule*, 2018, **2**, 764-777.
- S5 J. Pu, J. Li, Z. Shen, C. Zhong, J. Liu, H. Ma, J. Zhu, H. Zhang and P. V. Braun, *Adv. Funct. Mater.*, 2018, **28**, 1804133.